



NRCP
RESEARCH JOURNAL

Full Paper

Simulated Changes in the Phytoplankton Community Structure at the Subsurface Chlorophyll Maximum in the Philippine sea: Sensitivity Analysis and Possible Temperature Scenarios

Kristina S.A. Cordero-Bailey^{1*,2}, Jose de Leon², Laura T. David² and Aletta T. Yñiguez²

¹Department of Community and Environmental Resources, College of Human Ecology, University of the Philippines Los Baños, kscordero@up.edu.ph

²Marine Science Institute, University of the Philippines Diliman, jfdeleon@gmail.com, lt david@msi.upd.edu.ph, atyniguez@gmail.com

Our study simulated a size-structured phytoplankton community in the Philippine Sea to determine the factors that regulate the vertical phytoplankton distribution using a one-dimensional coupled physical-biological individual-based model in the Virtual Ecosystem Workbench (VEW) software. Three phytoplankton groups (pico-, nano- and microphytoplankton) were governed by specific metabolic and reproductive rates and simulated to be grazed on by copepods, which in turn were controlled by carnivorous zooplankton. Sensitivity analysis using three salinity scenarios (33, 34 and 36 Practical Salinity Units [PSU]) showed that nutrient availability drives the phytoplankton communities towards the end of the simulations, wherein only the 34 PSU simulation was able to recreate the Subsurface Chlorophyll Maximum (SCM) profile similar to the 2011 *in-situ* observation. Three temperature scenarios (+1.0°C, +2.0°C, +10.0°C) were then used to predict phytoplankton responses to changing temperature regimes. The scenarios predicted the SCM would develop deeper than the original simulation and a significant increase in the abundance of the dominant phytoplankton at the SCM, possibly affecting the higher trophic web or increasing the deep carbon export to deeper waters. Although the VEW software has been useful for investigations on plankton dynamics of global and specific regions, our study finds that the physical dynamics of the software is not attuned to simulate the highly variable Philippine Sea setting, limiting the model runs only to the drier months of the year. We suggest caution in the use of the version of the software as it needs restructuring to be more useful in such areas.

Keywords: phytoplankton community structure, individual-based model, sensitivity analysis, salinity, temperature scenarios



Article history

Received : April 4, 2024

Revised : July 10, 2024

Accepted: July 12, 2024

Introduction

Subsurface chlorophyll maximums (SCMs) are ubiquitous features of stratified oceans (Cullen 2015) occurring when nutrient availability at the euphotic depth are optimal to allow the proliferation of phytoplankton. Cullen (2015) referred it to the "Typical Stable Water Structure", highlighting that the interacting processes leading to water column stability contribute more to the formation of the SCM rather than environmental conditions per se. As such, tropical and subtropical waters with quasi-permanent stratification have been reported to have the SCM feature present year-round and are persistent throughout the day as long as conditions remain constant (Gong et al., 2014; Gong et al., 2015; Hense & Beckmann, 2008; Teira et al., 2005). As SCMs are undetected by remote sensing, primary production may be grossly underestimated when calculated solely from surface chlorophyll values (Weston et al., 2005; Probyn, Mitchell-Innes & Searson, 1995). Mechanisms governing the formation and maintenance of the SCMs have been studied since Riley et al. (1949) and these mechanisms, such as phytoplankton biomass aggregation at depth, photo-acclimation due to increase in chlorophyll pigment within the phytoplankton (Fennel & Boss, 2005), increased nutrient fluxes at the thermocline under high light conditions (Li & Hansell, 2017), are highly varied due to the complex SCM community and the external dynamics of physical forcing (Li et al., 2012; Cullen, 2015). Additionally, the removal of phytoplankton in the upper water column by grazing zooplankton may increase and improve incident light for phytoplankton growth at the mixed layer depth (Pannard et al., 2015).

Marine phytoplankton contribute to 50% world's photosynthesis (Falkowski et al., 1998; Field et al., 1988), therefore, the increased carbon sequestration at SCMs may also have a significant impact on climate by reducing the atmospheric CO₂ levels through the sinking of organic and inorganic matter to the deep ocean. In the past few decades, warming due to anthropogenic carbon emissions have been observed to influence phytoplankton dynamics and change in the phytoplankton composition (Ajani et al., 2021; Righetti et al., 2019). It is predicted to reduce phytoplankton productivity in tropical regions as a result of increased stratification

(Gittings et al., 2018; Thomas et al., 2012; O'Connor et al., 2009; Sommer & Lewandowska, 2011; Boyce et al., 2010; Intergovernmental Panel on Climate Change, 2014) while enhancing it at higher latitudes (Smith et al., 2007; McQuatters-Gollop et al., 2011; Taucher & Oschlies, 2011). Studies focused on the dynamics of plankton systems, whether from field observations or mathematical modelling, allow us to predict how plankton ecosystems would react to internal and external conditions including warming waters. The use of models for predicting plankton responses is well-documented with earth system models projecting a decrease in the global primary production which may be attributed to phytoplankton response to climate in the lower latitudes. (Franks, 2002; Woods, 2005; Cabre et al. 2014; Marinov et al. 2010). These responses may be brought about by increasing temperature, heavy precipitation and storm events which result in enhanced surface stratification or the intensification or weakening of nutrient upwelling. However, there are few models that predict how the vertical phytoplankton community would respond in a warming environment. Huisman et al. (2006) revealed how reduced mixing due to increased stratification induced oscillations and chaos in the phytoplankton in the SCM and increased productivity and deep carbon export.

The Lagrangian Ensemble (LE) metamodel was first presented by Woods and Onken (1982) as a hybrid of population- and individual-based models (IBM). The LE model uses a biologically-Lagrangian integration to follow the life history of each plankton class (phytoplankton, herbivorous and carnivorous zooplankton) and statistically calculate the population properties. The hybrid model combines equations from theoretical population ecology that enables prediction of changes in populations and primitive biological equations to describe each population in terms of single organisms (Woods 2005). The metamodel has been used to successfully predict ocean color (Liu & Woods, 2004), and create virtual ecosystems on various aspects of plankton dynamics (Wolf & Woods, 1988; Carlotti & Wolf, 1998; Miller et al. 1998; Woods & Barkmann 1995; Woods et al. 2005; Noguiera & Woods, 2005; Sinerchia et al. 2011). Model simulations were run in the Virtual Ecosystem Workbench (VEW) software (version 3.4) developed by Hinsley et al. (2007) which adheres strictly to LE modelling. The software creates a virtual mesocosm typically to a depth of 500m, extending into the permanent thermocline and this mesocosm is taken to represent 100km² of the mean conditions of the target area. VEW allows users to input the biological IBM model to be

used and integrates it to a physical model to allow the Lagrangian tracking of the plankters. Previous LE models cited including those run within VEW such as Lagrangian Ensemble Recruitment Model (LERM) (Sinerchia et al., 2012) were tested in Azores Island in the North Atlantic where net annual heat and salinity budget are zero. As the user has minimal control in the physical model, which is integrated in the software, this study attempted to see the applicability of VEW in the Philippine setting that annually encounters a wide range of salinity. It was determined that model results had to be limited only to the drier periods of the year (March to May) when the simulated physical parameters were most similar to actual conditions. *In-situ* data collection in 2011 and 2012 by Cordero-Bailey et al., (2021) coincided with this period.

The Philippine Sea is highly influenced by the northeast monsoon from November to February. Additionally, the region generally experiences quite a number of typhoons (~20) every year, with the past several years experiencing unusually strong storms (Category 3 or higher on Saffir-Simpson hurricane wind scale). Potential increase in temperature due to climate change may therefore affect both physical and biological features of this highly dynamic region. During two observational cruises in the Philippine Sea, Cordero-Bailey et al. (2021) found the cooler temperature accompanying the intrusion of the Kuroshio recirculation gyre in 2011 to be the driving factor in the higher chlorophyll levels and phytoplankton abundance in the region. However, their study sampled only net-phytoplankton (>20µm) and did not account for the smaller pico- and nanophytoplankton that could significantly contribute to the total phytoplankton community and primary production in the region. The aims of this study are to (1) test the sensitivity of VEW to recreate the formation of the SCM in the Philippine Sea and (2) determine the change in vertical plankton distribution in response to a hypothetical thermal stress. We simulated a size-structured phytoplankton community (pico-, nano- and microphytoplankton) using a coupled physical-biological individual-based model. One of the main limitations of the study was the lack of empirical phytoplankton data on the smaller class sizes (pico- and nanoplankton) for validation.

Methodology

Study Site

The Philippine Sea is located northeast of the island of Luzon, facing the Pacific Ocean (Figure 1). This

region is where the North Equatorial Current (NEC) bifurcates with the northward current feeding into the Kuroshio Current while the southward current feeds into the Mindanao current. As the NEC serves as an important pathway for heat and water mass exchange between the low- and mid-latitude North Pacific Ocean, its location therefore plays a crucial role in the large-ocean circulation and climate variability of the Pacific (Qiu et al. 2015; Lien et al. 2014; Talley et al. 2007).

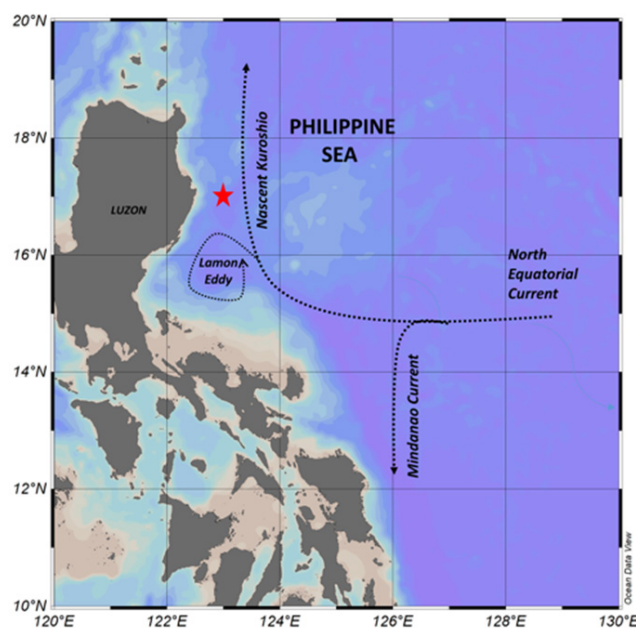


Figure 1. Location of model station (red star, 16.99°N, 123.00°E) in the Philippine Sea.

Physical Model

In this study, we only used model outputs for the Philippine Sea domain, simulated at a stationary point (16.99°N, 123.00°E). (Figure 1). Virtual Ecology Workbench (VEW) [version 3.4] creates a virtual mesocosm typically to a depth of 500m, extending into the permanent thermocline and this mesocosm is taken to represent 100km² of the mean conditions of the target area. The software uses the OCCAM global circulation model (<http://www.noc.soton.ac.uk/JRD/OCCAM/>) with a ¼° resolution. The boundary conditions comprise fluxes through the interface between atmosphere and ocean, at the top of the mesocosm. Fluxes that are unaffected by the state of the virtual ecosystem include the downward irradiance of sunlight (insolation), and the precipitation of water. VEW adopts the 25-waveband spectrum of Woods, Barkmann et al. (1984) and is forced by the monthly climatology of ERA-40 meteorological data (cloud cover at standard level, wind, temperature, humidity at standard height above sea level) and ERA40 fluxes (sensible heat, latent heat, net IR, momentum, precipitation).

Initial conditions for the physical model (temperature, salinity and density) were based on data retrieved by the Biogeochemical (BGC) Argo float #2902573 for January 2020 (Figure 2a). The depth of mixed layer depth (MLD) was set at 120m, based on previous *in-situ* observations made during 2011 and 2012. Initial chemical conditions (ammonium and nitrate) were also based on the *in-situ* cruise data (Figure 2b).

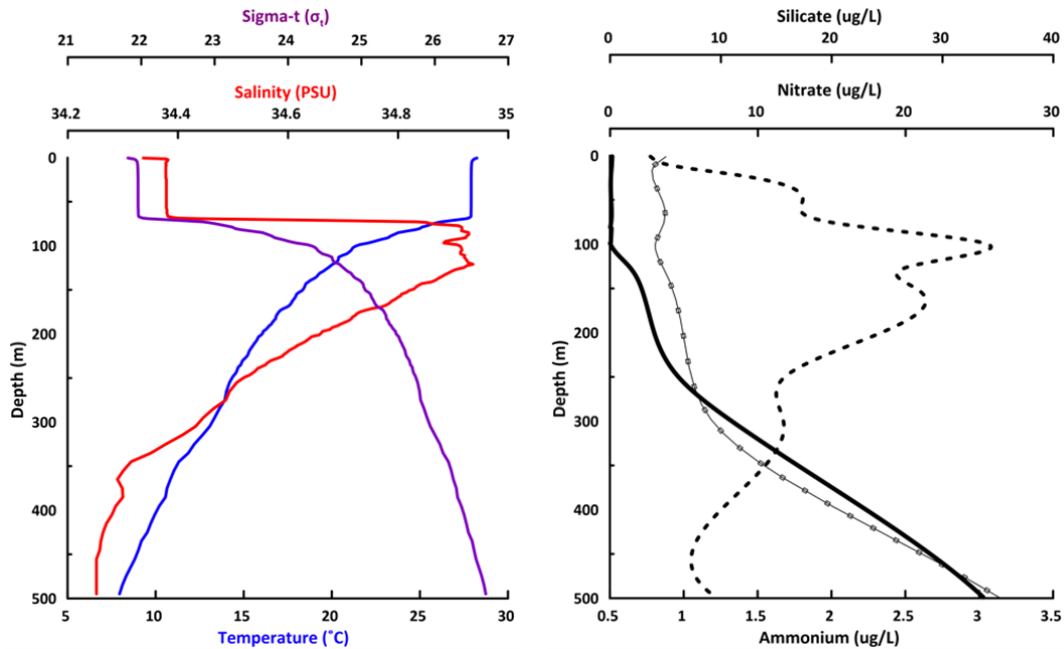


Figure 2. Initial parameters used for (a) temperature (blue), salinity (red), density (purple) and (b) silicate (dashed), nitrate (black solid), ammonium (solid with dots)

Initial runs of the full model were unsuccessful, and it was determined that the freshwater input during the SW monsoon was negatively affecting the physical model (Figure 3). Sensitivity analyses to determine the response of plankton communities were performed at three salinity conditions : (1) 34 Practical Salinity Units [PSU], simulating the initial conditions of the BGC-Argo float, (2) 33 PSU simulating wet/rainy conditions and (3) 36 PSU to simulate drier conditions when evaporation is increased. Results in the following section shall be presented in this particular order.

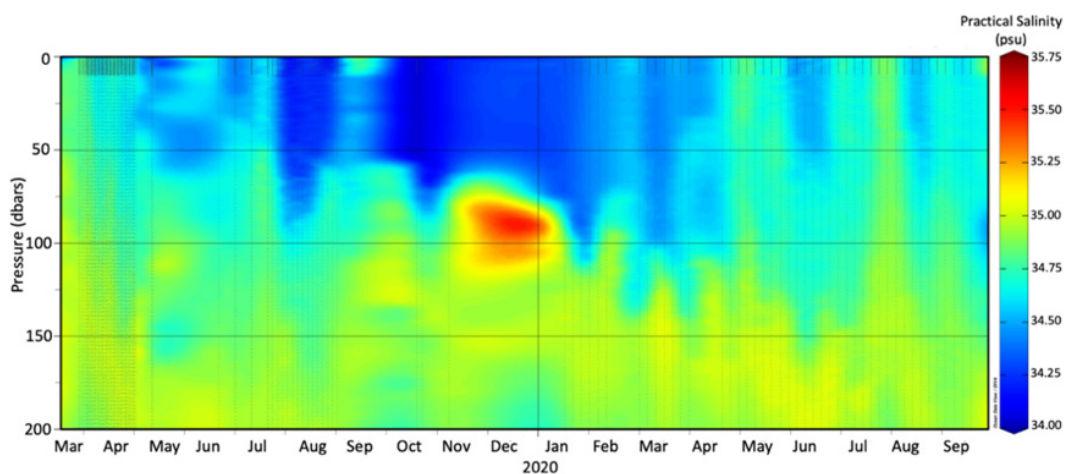


Figure 3. Salinity distribution from March 2019 to September 2020. Data retrieved from Biogeochemical (BGC)-Argo float # 2902573.

Figure 4 a,c and e display the modelled surface temperature, mixed layer depth (MLD) and windspeed. Figures 4b, d and f represents sea surface temperature from MODIS-A, MLD determined by the NASA Ocean Biogeochemical Model (NOBM) (Gregg & Rousseaux 2017) and wind speed processed by the Modern-Era Retrospective analysis for Research and Applications version 2 (MERRA-2) (GMAO 2015), respectively. The shallowing of the MLD can be seen to match the decrease in windspeed with an accompanying increase in temperature on March 1 (Day 60). Trends of modelled physical parameters are fairly similar to that observed data from March 1 (Day 60) until May 30 (Day 150). After this point, modelled parameters

continued increasing for temperature and MLD and decreasing for wind in spite of observed decrease in temperature and fluctuations in the mixed layer depth and wind speed during the southwest monsoon. These deviations could possibly be due to the complications within the physical module, similar to the effects of low salinity. From this, we determine that in the Philippine setting, the physical model of VEW appears to be only applicable in the drier months of the year and is unable to capture the natural variability of the region. Due to the uncertainties arising from the physical model, biological simulations only until May 30 (Day 150) were further analyzed.

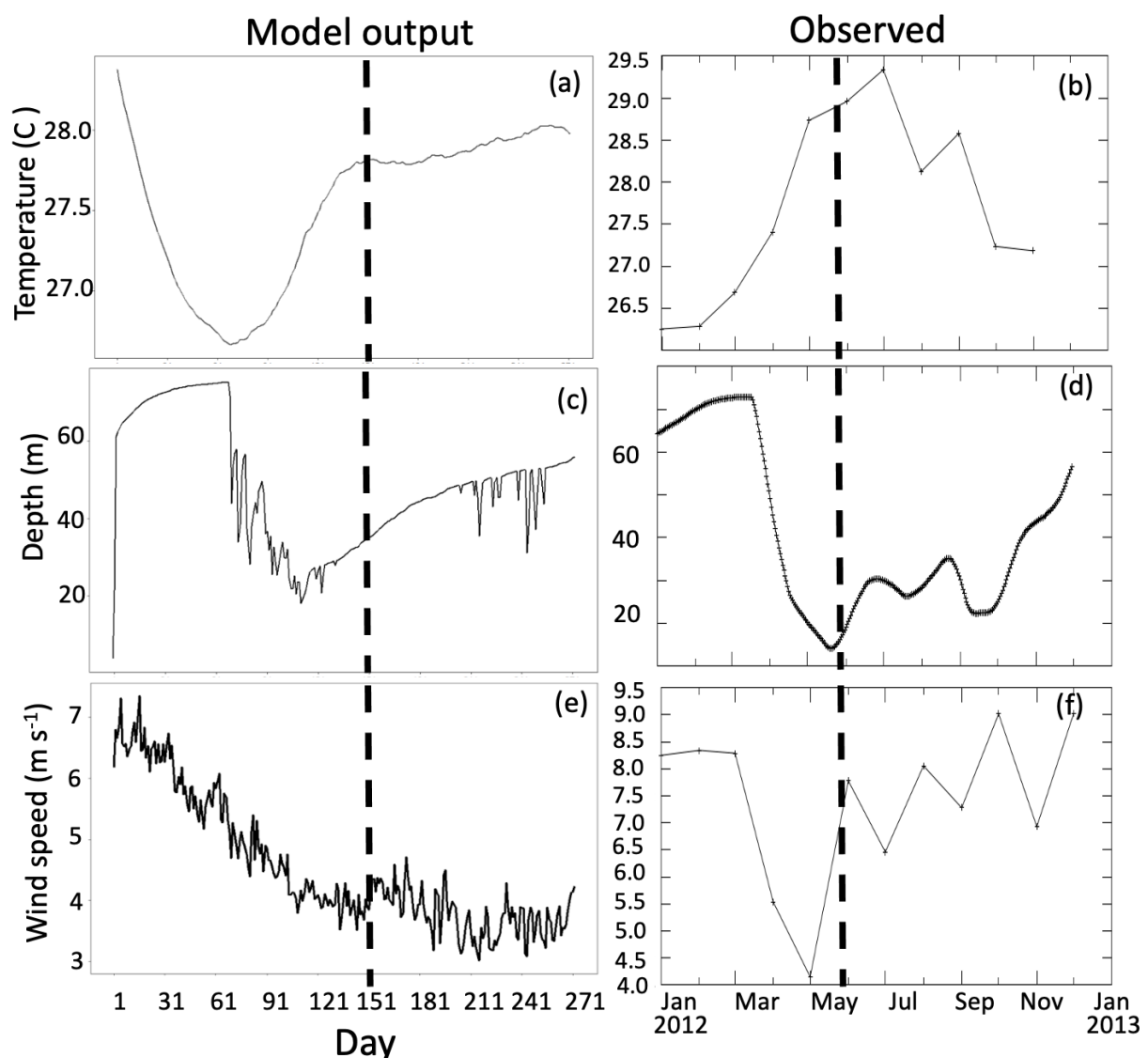


Figure 4. Surface temperature, mixed layer depth (MLD) and windspeed from the model simulation (a, b, c) compared to actual data from 2012 (d, e, f). Graphs for observed data were produced within the GES-DISC Interactive Online Visualization AND aNalysis Infrastructure (Giovanni) tool (<https://giovanni.gsfc.nasa.gov/giovanni/>).

Biological model

The biological model followed the framework of the LERM model by Sinerchia et al. (2012) incorporating the phytoplankton structure by Noguiera et al. (2007) (Figure 5). The model has seven components representing three sizes of phytoplankton - picophytoplankton (0-2µm estimated spherical diameter [ESD]), small eukaryotes (referred as nanophytoplankton) (2-20 µm ESD) and large eukaryotes (=microphytoplankton) (20-100 µm ESD); herbivorous zooplankton, and carnivorous zooplankton, and two forms of dissolved inorganic nitrogen (DIN): nitrate and ammonium.

Each phytoplankton type was initiated with 80 agents per meter, with 100 individuals per agent from the surface to 200m. The main difference among the three classes lies in their mass-specific metabolic rates with the small picoplankton having higher nutrient uptake and reproductive rates compare to the larger ones. In effect, sinking rates of the smaller cells are slower than their larger

counterparts.

All three phytoplankton classes were grazed by a copepod community that also have their own metabolic processes. The initial copepod population were set at 10 adult copepod agents every meter with 50 individuals per agent. This population was based on Herman (1983) who observed copepod concentrations of 100-500 m⁻³. The copepods in turn were preyed upon by carnivorous zooplankton, which represented trophic closure for the biological model. These carnivorous zooplankton were introduced at one agent per meter, with three individuals representing one agent for the upper 100m. Both herbivorous and carnivorous zooplankton actively performed diel vertical migration, i.e, they are able to move vertically during the day to avoid predation. Zooplankton remineralization and excretion released ammonium that was eventually incorporated to the Dissolved Inorganic Nitrogen (DIN) pool for availability during entrainment and/or upwelling.

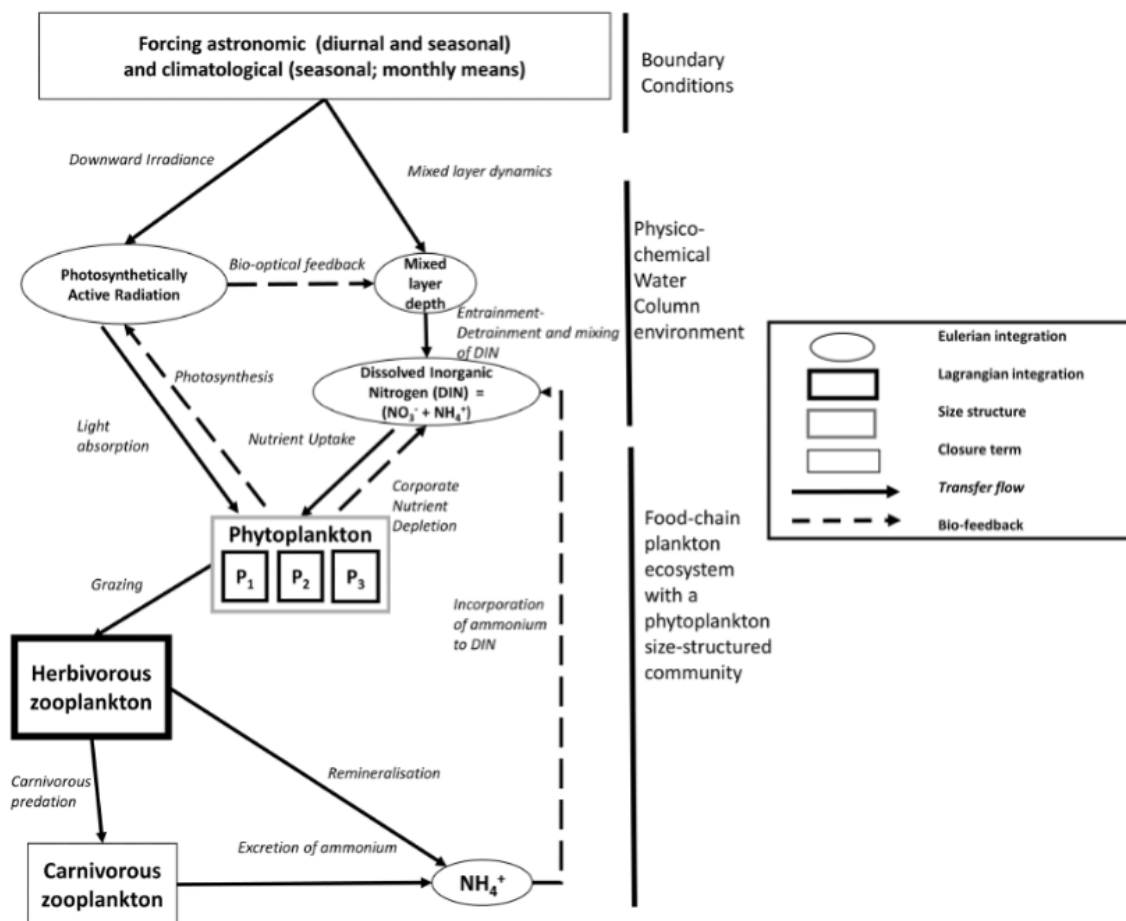


Figure 5. Biological model framework based on Sinerchia (2012). The three phytoplankton groups, represented as P1 (picophytoplankton), P2 (nanophytoplankton) and P3 (microphytoplankton), are fed on by herbivorous copepods which in turn are prey to carnivorous zooplankton.

The biological equations for each plankton class used in this model are elaborated in Sinerchia (2012) with the exclusion of the functional group representing top predators (squids) while parameters used to represent the size-dependent processes for reproduction and metabolism in the biological model are based on Noguiera and Woods 2006. From January 1 (Day 1) to March 9 (Day 68), the model showed uniform profiles within all phytoplankton classes from the surface to the MLD (Figure 6). We attribute this to the spin-up period

of the model to recreate the SCM feature. Therefore, to focus strictly on the changes in the vertical distribution, results of the simulation was further limited to March 10 (Day 69) to May 30 (Day 150), which corresponded to the 2011 and 2012 *in-situ* data collected by Cordero-Bailey (2021). Although zooplankton profiles showed copepods present at deeper depths, results for the copepod distribution will be limited to the euphotic layer to coincide with the SCM that were formed in the upper 200m.

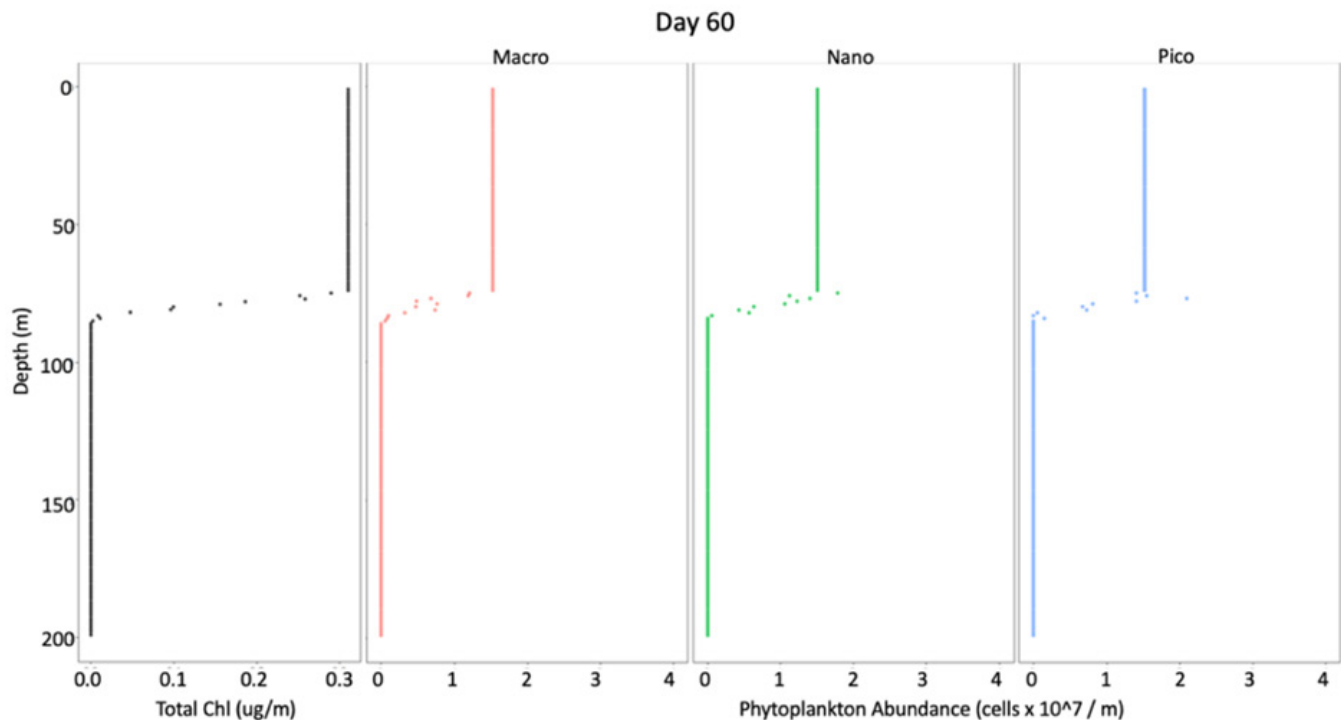


Figure 6. Profiles of phytoplankton classes were seen to be homogenous from the surface to the MLD from the start of the simulation until March 8 (Day 68).

The modelled vertical chlorophyll distribution was compared to chlorophyll data from the Biogeochemical-Argo (BGC-Argo) float #2902753 released by the China Argo Program in March 2019.

Temperature scenarios

Development of VEW intended to allow exogenous changes (biological/ chemical/ physical) to simulate what-if events (VEW handbook 2007). However, physical changes are complicated as the physical variables (density, irradiance, salinity, temperature) were inherently part of the physical module and thus, the feedback effects would translate to changes in the physics coding, possibly producing unrealistic biological results. The VEW development

team was only able to provide a mechanism that enabled biological changes due to temperature events without any adverse reaction to the MLD. Other physical variables for other scenarios were unfortunately inoperable. For this study, events simulating increasing temperature were introduced to determine how temperature influences the formation and maintenance of the SCM. Several different temperature scenarios (+1.0°C, +2.0°C, +10.0°C) at 34 PSU, were tested to simulate an increase in temperature in the study area. These temperature scenarios were chosen to replicate moderate- (RCP 4.5) and high-emission (RCP 8.5) projections by the Intergovernmental Panel on Climate Change (2007).

Results

Sensitivity analysis

Simulated mixed layer depths and nutrient profiles

Figure 7 shows the modelled mixed layer depths (MLD) at the 34, 33 and 36 PSU. We can see that

the thermocline depth varies at the start of each simulation. At 34PSU, it is seen to begin around 75m while at 36PSU, it is shallower at 68m. As the simulations progress, we see that the thermocline depth remains relatively constant, regardless of the wetter (33PSU) or drier (36PSU) conditions.

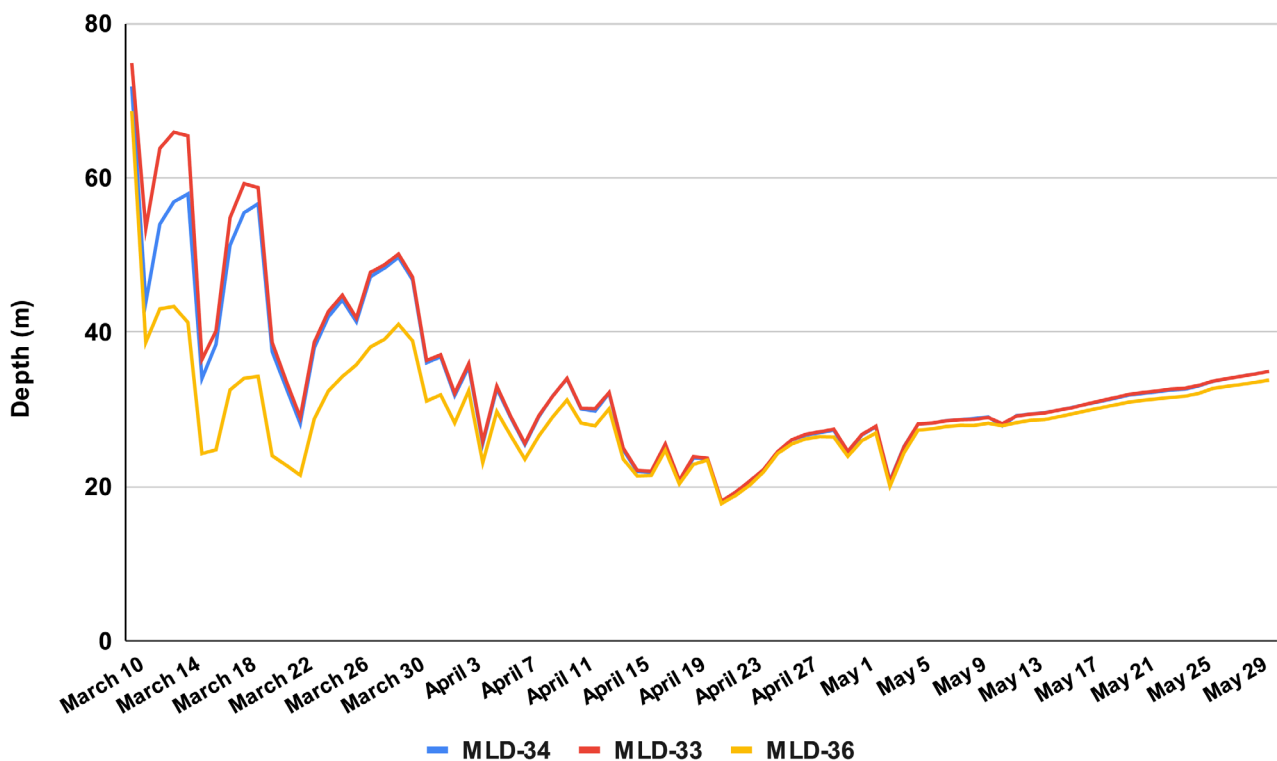


Figure 7. Profiles of mixed layer depths simulated at 34 PSU, 33 PSU (wet) and 36 PSU (dry).

Figure 8 shows the modelled nitrate (NO₃) and ammonium (NH₄) available in the water column. NO₃ profiles (Figure 8a, c, e) remained fairly constant with depletion from the surface to depths of 100m in all simulated salinities. The nutricline for ammonium profiles begin at 75m, with the lowest concentrations in the 33PSU simulation (Figure 8b, d, f). It should be noted that from April 30 onwards at all salinities, ammonium can be seen to decrease between 75-100m. Nutrients were highest after these depths, simulating naturally nutrient-rich bottom waters.

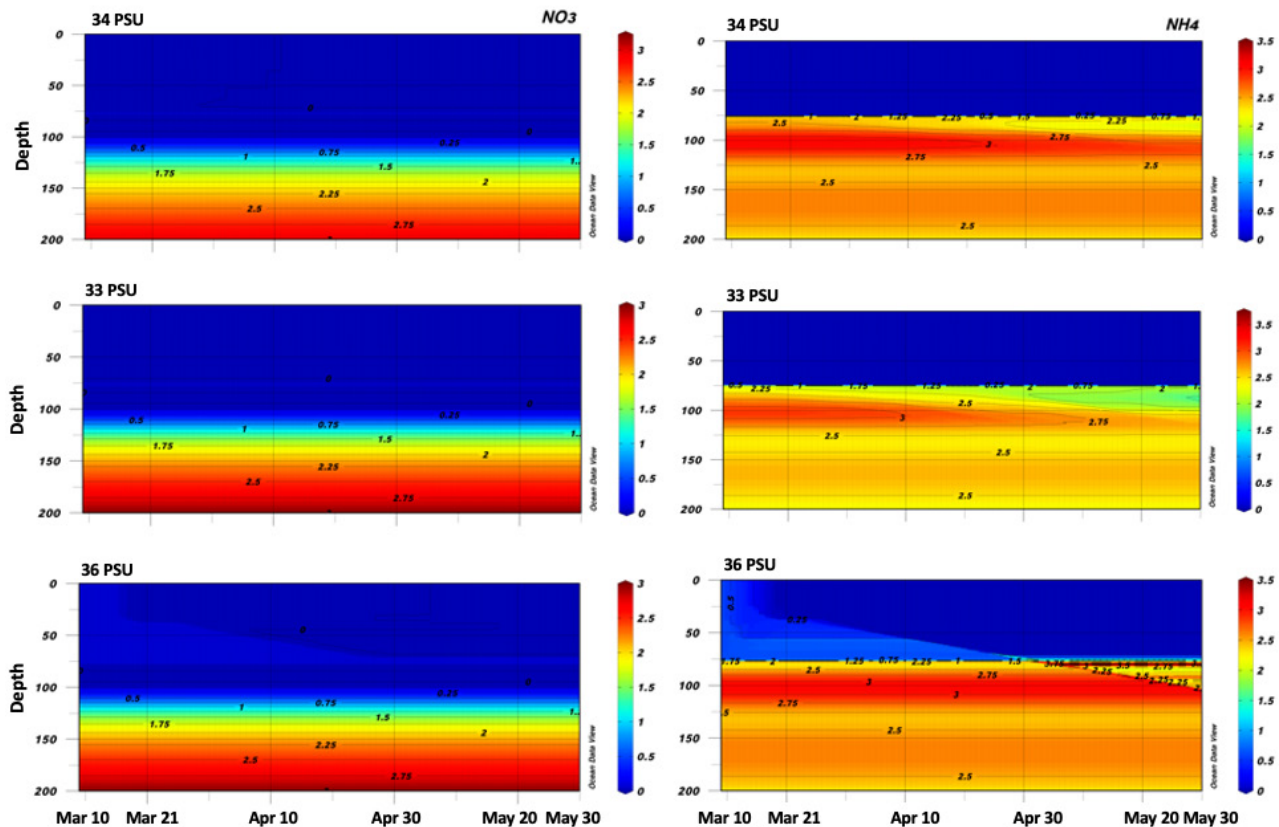


Figure 8. Nutrient profiles simulated at varying salinities. Nitrate (NO₃) are seen to be similar in all simulations but ammonium (NH₄) vary in concentration at the nutricline, particularly after April 30.

Vertical plankton variation

In the first simulation, the formation of a subsurface maximum begins on March 10 and is fully formed by March 31 (Figure 9a). The peak of the SCM concentration is seen around May 10 at 0.75 mg m⁻³ at around 100m. The simulation under 33PSU shows a similar pattern and similar depth, but total Chl-a in the SCM layer ranged from 1–4 mg m⁻³ (Figure 9b). In the third simulation at 36PSU, the SCM is formed later on March 21 at a shallower depth of 50m. (Figure 9c). The peak SCM concentration was shallower around 75m on April 30, with the highest total Chl-a range (10-40 mg m⁻³). It can be seen

that the observed chlorophyll in March showed a distinct SCM to be present at around 100-110m, with fluctuation of the SCM to depths of 150m in late April and June 2019 (Figure 9d). All the three modelled Chl-a distribution appeared to capture the observed distribution towards the end of the simulation. The following section shall present the vertical phytoplankton distribution in more detail.

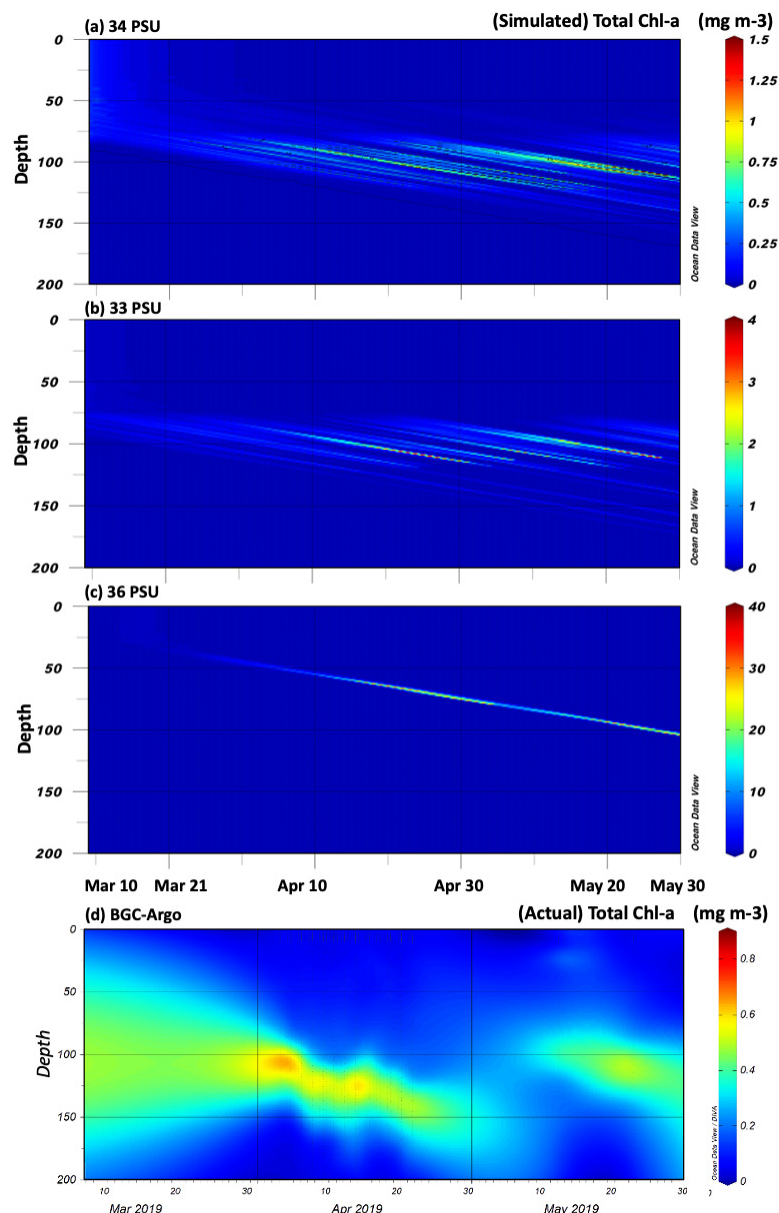


Figure 9. Simulated total chlorophyll in all phytoplankton at (a) 34 PSU (b) 33 PSU (c) 36 PSU compared to observed vertical chlorophyll distribution (d) from BGC-Argo (Mar-May 2019). Chl-a range in the latter two simulations are noticeably larger due to the increased phytoplankton abundance.

In the first simulation (34PSU) on March 10, a chlorophyll peak (0.247 mg m^{-3}) begins to develop at 67m, dominated by picophytoplankton (Figure 10a). As the profile develops into a normal distribution, the SCM was modelled to form deeper in the water column, with nano- and microphytoplankton alternating as the dominant phytoplankton. From April 30 (Day 120) onwards, the small picophytoplankton ($8.62 \times 10^7 \text{ indl m}^{-2}$) dominated the SCM at depths between 102-123m. We also looked into the potential influence of copepod grazing on the phytoplankton community. During the entire simulation, there was a uniform maximum layer with the highest copepod abundance found from the surface to a depth of $\sim 30\text{m}$. Below this surface layer, copepod layers ranging from 7-26m (average 13m) were present. From April 20 onwards,

a minimum of four copepod layers at varying concentrations and depths were observed in the copepod profiles, of which one layer would coincide with the peak depth of the SCM ($\pm 5\text{m}$).

In the 33PSU simulation, the SCM formed at similar depths to the first simulation. SCM peak (0.196 mg m^{-3}) was already distinct on March 10, dominated by nanophytoplankton (Figure 10b). By April 30 (Day 120), the microphytoplankton ($2.29 \times 10^8 \text{ indl m}^{-2}$) dominated the SCM peak (2.42 mg m^{-3}) at 115m. At the end of the simulation (May 30), the nanophytoplankton ($6.94 \times 10^7 \text{ indl m}^{-2}$) dominated the SCM again at 103m. The copepod distribution during the simulation was distinctly different from the first run with the copepod layers forming deeper in the water column, usually far below the SCM. At

the end of the simulation (May 30/Day 150), there was a copepod peak (4697 indl m⁻²) observed at 191m.

In the 36PSU simulation (Figure 10c), the profiles were distinctly different from the previous runs in terms of concentration of Chl-a and abundance of the phytoplankton groups. On March 10 (Day 69), there is no SCM peak, with a uniform profile from the surface at 0.281 mg m⁻³, dominated by

picophytoplankton (1.25×10^7 indl m⁻²). SCM peak formed fully only on March 21 (Day 80) (Figure 9c). On April 30 (day 120), the SCM (35.000 mg m^{-3}) was observed at 76m, dominated by picophytoplankton with 4.88×10^9 indl m⁻². The simulation ended with a deep SCM (37.720 mg m^{-3}) at 105m, with a shift to microphytoplankton (4.16×10^9 indl m⁻²). Copepod layers were normally observed just below the SCM peaks in this simulation, with the peak copepods (4160 indl m^{-2}) at 128m on May 30.

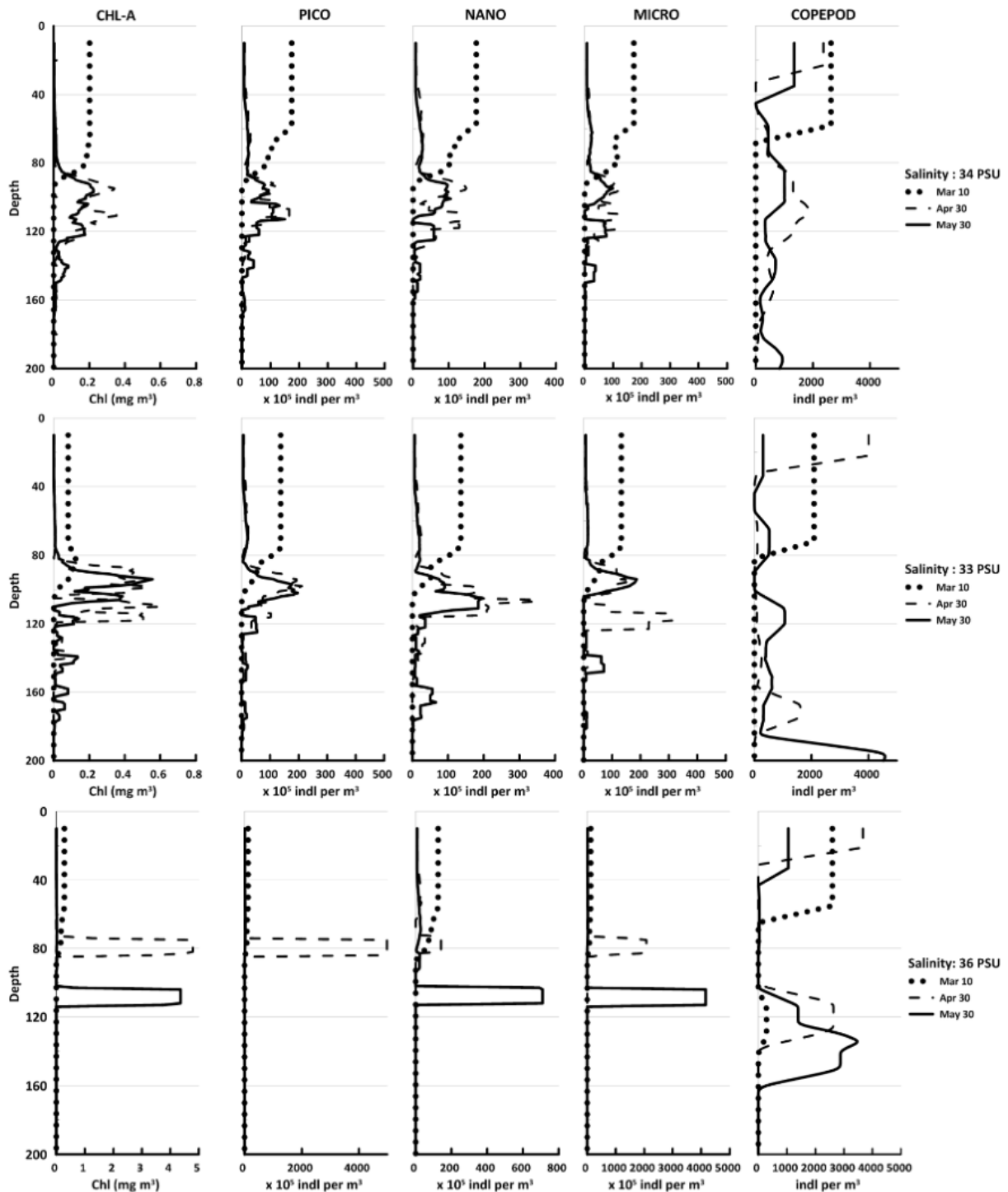


Figure 10. Simulation of vertical plankton distribution [Chl, picophytoplankton, nanophytoplankton, microphytoplankton and copepod] at (a) 34 PSU (b) 33 PSU (c) 36 PSU.

The SCM on May 30 were similarly formed between 90-100m in all three scenarios, but only the concentration at the SCM in the 34PSU simulation is comparable to the mean SCM concentration from the in-situ observations (Figure 11). Henceforth, the temperature scenarios presented in the following section uses 34PSU as the baseline salinity.

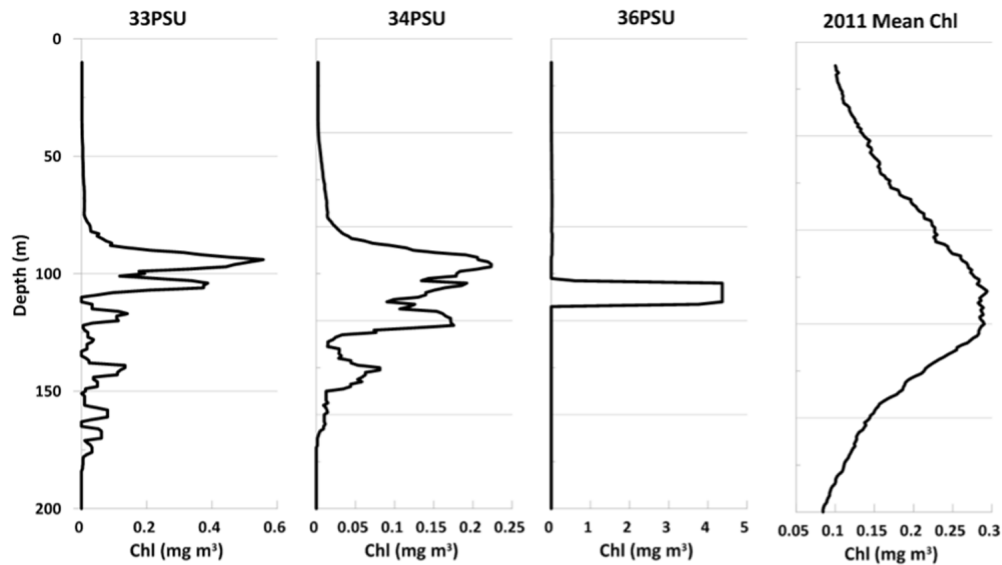


Figure 11. Simulated chlorophyll profiles on May 30 (Day 150) at different salinities compared to the mean chlorophyll profile from in-situ observations in 2011.

Temperature Scenarios

Figure 12 shows the resulting temperature distribution for five temperature scenarios (+1°C, +2°C and 10°C) performed at 34PSU. The thermocline was observed between 75-100m with the variations occurring conservatively (~0.5°C) between temperature scenarios with the steepest thermocline in the +10°C simulation.

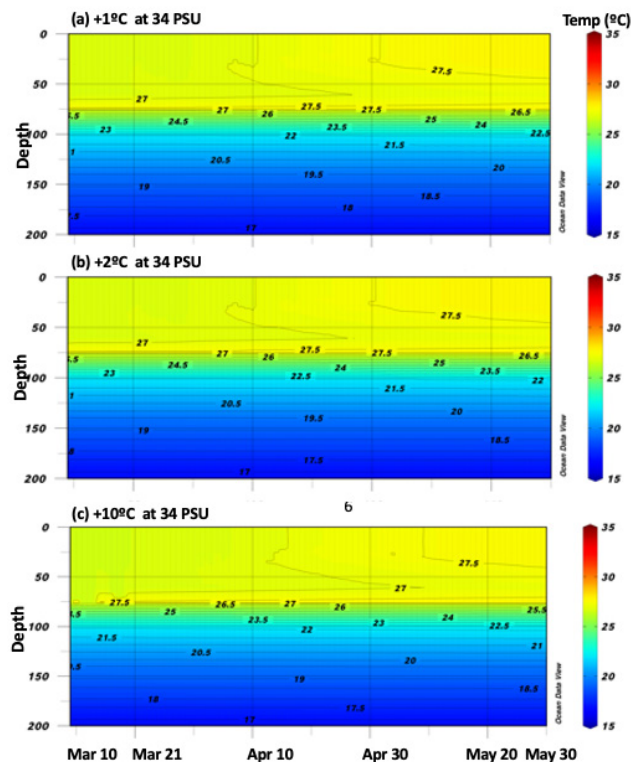


Figure 12. Simulated temperature distribution under three temperature increase (a) 1°C, (b) +2°C and (c) 10°C. The impact of hypothetical increase was gradual in all simulations, implying the buffering effect within the modelled mesocosm that could be distributing the temperature increase from the surface to the deeper layers.

Table 1 provides the summary of the different temperature and salinity scenarios. The SCM in the temperature scenarios at 34PSU also developed on March 10, as in the original simulation. These scenarios showed that the SCM formed deeper than 104m (original simulation) with the extreme +10°C at 226m. With the 1.0°C temperature increase, the model simulated a shift to the microphytoplankton class with a significant increase in abundance to 1.38×10^{10} indl m⁻² at 133m on May 30, almost three orders of magnitude compared to the original run. In the 2.0°C increase, abundance in the picophytoplankton at the peak depth increased to

4.45×10^{10} indl m⁻² by May 30. These abundances led to the high SCM concentrations of 156.119 mg m⁻³ and 279.557mg m⁻³ respectively. Copepods only peaked coincidentally with the SCM in the +2.0°C simulation, while there was a copepod layer present at the SCM in the +1.0°C. The extreme +10°C scenario showed deeper SCM at 226m by May 30, but SCM concentration of only 0.745 mg m⁻³, of which nano- and microphytoplankton shared dominance of 3.09×10^7 indl m⁻², less than the total abundance of the original (34PSU) simulation. None of the copepod layers coincided with the deep SCM.

Table 1. Summary of plankton response at the end of simulation run (May 30) in different temperature scenarios.

	34 PSU (baseline)	+ 1°C	+2°C	+ 10°C
Peak SCM Depth (May 30 / Day 150)	104	134	125	226
SCM conc (mg/m ³)	0.670	156.119	279.557	0.745
Dominant group at SCM (May 30 / Day 150)	Pico (100%)	Micro (100%)	Pico (100%)	Nano (50%) Micro (50%)
Abundance of dominant group (indl/m ²)	8.62×10^7	1.86×10^{10}	4.45×10^{10}	3.09×10^7
Depth of Copepod layers (m)	1-33 52-69 80-95 105-115 185-192	1-34 127-143 186-1921	1-22 103-117 125-140	1-35 37-73 110-161
Copepod Abundance per layer (indl/m ²)	1343 436 1002 328 934	1313 482 4810	32222 118 3314	415 51 6067

Note: Percentages indicate composition of dominant plankton group while depths in bold italics indicate the location of the SCM depth.

Discussion

Sensitivity analysis

The 34PSU simulation provides new information on the dynamics of the SCM in the Philippine Sea. Under the BGC-Argo conditions (34PSU), the model simulated the formation of the SCM in three phases: Phase 1 (March 10-11), the decrease in winds and turbulent mixing allowed the small picophytoplankton to be the first class to proliferate at the SCM, taking advantage of the high nutrients from below at the mixed layer depth. During Phase 2 (March 12 – April 30), the phytoplankton

were actively competing for nutrient resources as the dominant phytoplankton class varied as the model progressed. In the last phase (April 30 – May 30), the picophytoplankton dominated again, accompanying an obvious decrease in ammonium concentration. This could indicate the recycled nutrient was driving the phytoplankton growth. This phase of the simulation corresponds to the end of the inter-monsoon period (April-May) in the region where there are low wind conditions and thereby, less mixing to induce the introduction of new nutrients from below.

The 33PSU simulation recreates wet/rainy condition and the model supported cooler temperatures, which in turn appeared to be more favorable for all the phytoplankton classes as their abundances, particularly the nanophytoplankton by May 30, increased at the SCM compared to 34PSU. The simulation appears to be similar to conditions during the 2011 cruise reported by Gordon et al. (2014), Cabrera et al. (2015) and Cordero-Bailey et al. (2021), wherein cooler temperatures corresponded to increase in chlorophyll and phytoplankton abundances.

In the simulation for drier conditions (36PSU), the SCM formed later (March 21) that coincides with the NH_4 depletion to a depth of 50m. Warmer temperatures was highly favored initially by picophytoplankton on April 30, and by the microphytoplankton at the end of the simulation, again driven by NH_4 depletion. Notably, the abundances of the two phytoplankton types were three orders of magnitude higher than the 34PSU simulation. The *in-situ* 2012 observation of Cabrera et al. (2015) and Cordero-Bailey et al. (2021) showed higher salinities from the warm North Equatorial Current dampened the total chlorophyll at the SCM and also shifted to more diatom species. The ultimate shift to the larger microphytoplankton was replicated by the simulation but there is a discrepancy between the observed and simulated total Chl-a and abundances, possibly due to specific Chl-a composition of the phytoplankton species. The model had only assume the same Chl-a composition for each size class which is highly unlikely in reality.

Although the simulations for the wetter (33PSU) and drier (36PSU) conditions appear to relate to the *in-situ* observations in terms of the phytoplankton community change, we determined only the 34PSU simulation to have closely recreate the 2011 *in-situ* condition in terms of the SCM depth and concentration, while revealing the importance of the small picophytoplankton within the plankton ecosystem. Simulations under 32PSU failed to progress due to the salinity instability of the physical model.

The model simulated an important aspect that the observational cruises or the BGC-Argo data were not able to capture due to their respective sampling limitations - the dominance of the picophytoplankton at the SCM. Furthermore, the model showed that this small phytoplankton community is sustained mainly by recycled nutrients, particularly ammonium

which is specified as a by-product of the nitrate cycle in the biophysical model. Picophytoplankton are the smallest component of the phytoplankton community and they represent an important component of the microbial loop which is the trophic pathway of carbon and nutrient cycling by virtue of bacteria (Azam et al. 1983). Due to the decrease availability of nutrients in oligotrophic systems, such as the Philippine Sea, the microbial loop is important as it augments primary production by incorporating dissolved organic carbon (DOC) in bacterial biomass and returning the energy to the conventional planktonic food chain. Cordero-Bailey et al. (2021) and Chen et al. (2014) similarly presented net-phytoplankton composition for the study area and both studies did not sample for the small picophytoplankton, thus we are unable to directly validate the dominance or shifts of the phytoplankton size-classes. Globally, the contribution of picophytoplankton in oligotrophic waters has been reported to be as high as 40-45% of the total Chl-a biomass (Maranon et al., 2012; Lopez-Urrutia & Moran 2015; Uitz et al., 2006) while Takahashi & Tori (1984) showed empirically that picophytoplankton in the nearby South China Sea and northwestern Pacific Ocean contained 70% Chl-a in both surface water and the SCM.

Thompson et al. (2015) looked into the potential effects of precipitation on the phytoplankton ecology and their findings highlighted that the phytoplankton response is highly dependent on season and region, generally with more positive response for chlorophytes (pico- and nanophytoplankton) to increased precipitation in summer (warmer) conditions and a decrease in chlorophytes in dry and drying ecosystems during dry springs and summers. Our current model appeared to capture similar phytoplankton shifts as Thompson et al. (2015) but we acknowledge the caveat in precisely predicting the phytoplankton abundance at higher salinities.

Zooplankton grazing

In all simulations, adult copepods were distributed in distinct layers in the simulated water column. Herman (1983) looked into the vertical distribution of copepods vis-à-vis the chlorophyll and primary production profiles in Baffin Bay, Greenland. Peak copepod layers of *Calanus finmarchicus* and *C. gracialis* were found to be 3-5 m above the SCM but for other species such as the *Calanus hyberboreus*, the peak layers occurred below the SCM or deeper. In our study, although some copepod layers coincided

with the SCM peak, the copepod layer at the SCM did not have the highest abundance relative to other depths. This implies the copepods exert minimal to no control over the phytoplankton distribution as they were found in layers either above or below the SCM. In a recent study by Chenillat et al. (2021), their sensitivity analysis showed that size clustering of zooplankton may drive patterns and dominance within the phytoplankton community structure. However, our model did not capture such patterns as the herbivorous zooplankton was represented by only one size class. This may be an important feature that could be included to improve the model and the different sizes and copepod stages consume all size spectrum of phytoplankton (Jaggadesan et al., 2017; Gifford & Dag 1988; Banse 1994).

Moeller et al. (2019) studied the importance of top-down control in the formation of the SCM and they found that in clear waters when light penetrates deep into the nutricline, light-dependent grazing (top-down control) may be also an important mechanism influencing the depth or location in combination with available nutrients (bottom-up control). Our results show that the model is attuned more to the latter control (bottom-up) with the phytoplankton groups competing for nutrients from the deeper layers at the MLD.

Temperature scenarios

The three temperature scenarios showed distinctly different results from the base simulation (34PSU). The scenarios under 34PSU all resulted in deeper SCMs, which can be expected in a warming ocean wherein an increased surface temperature would decrease turbulence and/or mixing in the upper mixed layer and reduce uplift of nutrient-rich bottom waters (Finkel et al., 2010), resulting in a more stratified open ocean. Each scenario had different outcomes in the concentration at the SCM and abundance of the dominant phytoplankton group. The +1°C scenario observed a threefold shift to large microphytoplankton that could cascade to a trophic shift in the higher food web (Acevedo-Trejos et al., 2015). The 2°C resulted in the opposite spectrum wherein the growth of small cells was enhanced and this direct effect of temperature of the phytoplankton growth have been empirically observed (Lewandowska et al., 2014; Righetti et al., 2019; Peter & Sommer, 2012; Rasconi et al., 2017; Mesquita et al., 2020). The threefold increase in picoplankton abundance at the SCM indicate that the population can be sustained by two processes: (1) reliance on recycled nutrients (ammonium), as discussed in the previous section, or (2) increased

availability of nutrients from below the thermocline. Xiu et al. (2018) simulated that higher sea surface temperature in the future could potentially increase alongshore wind and coastal upwelling along the California coast. However, our simulations were not able to replicate fluctuations in wind conditions resulting from the hypothetical increase in temperature. Therefore, we can only surmise from our findings that the 2°C increase further enhanced conditions for the smaller phytoplankton to depend on ammonium within the system. Conventionally, community shifts to smaller sized phytoplankton has been anticipated to decrease overall primary productivity (Behrenfeld et al., 2006; Moran et al., 2010). However, Richardson and Johnson (2007) posed the aggregation of the abundant smaller phytoplankton in marine snow and consumption of these organic aggregates by zooplankton may have larger implications in terms of potential carbon export than previously thought. Their concept of the increased contribution of picophytoplankton to the carbon flux initiates vast opportunities for future validation studies.

The extreme +10°C simulation resulted in the deepest SCM at 226m, but total phytoplankton abundance was even less than the total abundance in the original (34PSU) simulation. The model anticipates the tolerance of the phytoplankton groups to extreme temperature by moving deeper into the water column as increased stratification could reduce the upwelling of nutrients from below the mixed layer depth. Thomas et al. (2017) modelled the population growth of the marine diatom, *Thalassiosira pseudonana*, that may be dependent on the temperature-nutrient interaction and found that the simultaneous increase in temperature and nutrient deprivation may lead to a greater decrease in primary productivity rather than the separate effects of these factors. As these simulations only accounted for the changes in temperature, the results showed that the phytoplankton may persist given that base nutrient conditions are constant.

Global warming influences phytoplankton dynamics, changing phytoplankton composition and biomass in the oceans (Defriez et al. 2016; Ajani et al. 2020; Chust et al. 2014). The three scenarios had varying outcomes in terms of the dominant phytoplankton group at the end of the test periods. These scenarios may either inducing a trophic shift in the food web or enhancing the deep carbon export (Huisman et al 2006; Richardson & Jackson 2007). The scenarios would most likely have cascading effects on primary and export production in the region. The

temperature scenarios reveal that predictions of a future warming climate may differ, depending on intensity of the increase in temperature as the stress fundamentally links growth rate, nutrient and light harvesting capabilities of the various phytoplankton classes. Considering that the changing climate has other compounding impacts on the ocean such as ocean acidification from increased atmospheric carbon dioxide that our model does not address, the final outcome of such multiple influences remains difficult to predict given the limitations of the software.

Limitation of the software

Although the VEW offers a tool allowing biological oceanographers to recreate and focus on the dynamics of plankton systems, the major limitation of the current version of the software appears to be the inability to simulate the complex physical and biological dynamics of a highly variable region such as the Philippine Sea. As such, these results and following conclusions should be considered with caution. Although we were unable to account for seasonal plankton variability, particularly during wet monsoon season wherein Cordero-Bailey et al. (2022) found higher integrated chlorophyll biomass with shallower SCMs following strong typhoon events, our results show that the software is capable to provide insights in the mechanisms of the phytoplankton communities. We highly recommend the restructuring and reconfiguring of the physical model of the VEW software to ensure that accurate simulations on the vertical biological patterns in the light of changing climate conditions.

It should be noted that certain factors that could have contributed to the formation and maintenance of the SCM such as light availability and zooplankton sinking were not considered. We acknowledge that factors such as these may alter system outcomes and thus should be highly considered in future studies.

Conclusion

Our model simulations show that the Virtual Ecosystem Workbench (VEW) appears to best recreate the phytoplankton community only during the drier months (March to May) in the Philippine Sea. In general, salinity scenarios showed that the model was able to recreate realistic response of the phytoplankton communities at 34PSU and the simulations indicates that nutrient availability may control the location, diversity and dominance of phytoplankton at depth. Temperature scenarios

gave distinctly different results: temperature increases may result in deeper SCMs with varying phytoplankton groups dominating the maximum layer. These simulations indicate that phytoplankton response to a warming climate can be variable and different processes can come into play under different scenarios.

Acknowledgments

Funding support for the research cruises was provided by the Office of Naval Research (ONR) Grant No. N62909-10-1-7126. We are grateful for the support and assistance of the crew and officers of the R/V Roger Revelle, volunteers and students that were actively involved in the two cruises. During the writing of the study, K.S.A.C-B. received financial support from the Department of Science and Technology – Science Education Institute (DOST-SEI) Accelerated Science and Technology Human Resource Development Program Scholarship, University of the Philippines In-House Project and the Coral Reef Visualization and Assessment program under the Dept. of Environmental and Natural Resources-Bureau of Biodiversity Management.

Authors Contribution

K.S.A.C-B. contributed in conceptualization, methodology, analysis and visualization, writing-manuscript preparation and final editing. **J.dL.** assisted in the model simulation while **A.T.Y.** and **L.T.D.** were in charge of supervision, reviewing and editing of the manuscript.

Declaration of interests

The authors declare that they have no known competing financial interests or personal relationships that could have appeared to influence the work reported in this paper.

Ethical Statement

The authors consciously assure that for the manuscript "Simulated Changes in the phytoplankton community structure at the subsurface chlorophyll maximum in the Philippine Sea : sensitivity analysis and possible temperature scenarios", the following are fulfilled:

- 1) This material is the authors' own original work, which has not been previously published elsewhere.
- 2) The paper is not currently being considered for

publication elsewhere.

3) The paper reflects the authors' own research and analysis in a truthful and complete manner.

4) The paper properly credits the meaningful contributions of co-authors and co-researchers.

5) The results are appropriately placed in the context of prior and existing research.

6) All sources used are properly disclosed.

7) All authors have been personally and actively involved in substantial work leading to the paper and will take public responsibility for its content.

References

- Acevedo-Trejos, E., Brandt, G., Bruggeman, J., & Merico, A. (2015). Mechanisms shaping size structure and functional diversity of phytoplankton communities in the ocean. *Scientific reports*, 5, 8918. <https://doi.org/10.1038/srep08918>
- Ajani, P. A., Davies, C. H., Eriksen, R. S., & Richardson, A. J. (2020). Global warming impacts micro-phytoplankton at a long-term Pacific Ocean coastal station. *Frontiers in Marine Science*, 7, 878. <https://doi.org/10.3389/fmars.2020.576011>
- Azam, F., Fenchel, T., Field, J. G., Gray, J. S., Meyer-Reil, L. A., & Thingstad, F. J. M. E. P. S. (1983). The ecological role of water-column microbes in the sea. *Marine ecology progress series. Oldendorf*, 10(3), 257-263. <https://doi.org/10.3354/meps010257>
- Behrenfeld, M., O'Malley, R., Siegel, D., McClain, J., Sarmiento, J., Feldman, G., Milligan, A., Falkowski, P., Letelier, R., & Boss, E. (2006). Climate-driven trends in contemporary ocean productivity. *Nature*, 444, 752-755 <https://doi.org/10.1038/nature05317>
- Boyce, D., Lewis, M. & Worm, B. (2010). Global phytoplankton decline over the past century. *Nature*, 466, 591-596 <https://doi.org/10.1038/nature09268>
- Cabré, A., Marinov, I., & Leung, S. (2015). Consistent global responses of marine ecosystems to future climate change across the IPCC AR5 earth system models. *Climate Dynamics*, 45(5), 1253-1280. <https://doi.org/10.1007/s00382-014-2374-3>
- Cabrera, O.C., Villanoy, C.L., Alabia, I.D. and Gordon, A.L., (2015). Shifts in Chlorophyll a off Eastern Luzon, Philippines, Associated with the North Equatorial Current Bifurcation Latitude. *Oceanography*, 28(4), pp.46-53. <https://doi.org/10.5670/oceanog.2015.80>
- Carlotti, F., & Wolf, U. (1998). A Lagrangian Ensemble model of *Calanus finmarchicus* coupled with a 1-D ecosystem model. *Fisheries Oceanography*, 7, 191-204. <https://doi.org/10.1046/j.1365-2419.1998.00085.x>
- Chenillat F, Rivière P, Ohman MD (2021). On the sensitivity of plankton ecosystem models to the formulation of zooplankton grazing. *PLoS ONE* 16(5). <https://doi.org/10.1371/journal.pone.0252033>
- Chust, G., Allen, J. I., Bopp, L., Schrum, C., Holt, J., Tsiaras, K., ... & Irigoien, X. (2014). Biomass changes and trophic amplification of plankton in a warmer ocean. *Global Change Biology*, 20(7), 2124-2139. <https://doi.org/10.1111/gcb.12562>
- Cordero-Bailey, K., Bollozos, I. S. F., Palermo, J. D. H., Silvano, K. M., Escobar, M. T. L., Jacinto, G. S., ... & Yñiguez, A. T. (2021). Characterizing the vertical phytoplankton distribution in the Philippine Sea off the northeastern coast of Luzon. *Estuarine, Coastal and Shelf Science*, 254, 107322. <https://doi.org/10.1016/j.ecss.2021.107322>
- Cordero-Bailey, K. S., Almo, A. T., David, L. T., & Yñiguez, A. T. (2022). Estimation of the vertical phytoplankton distribution in the Philippine Sea: Influence of turbulence following passage of typhoons. *Regional Studies in Marine Science*, 56, 102659. <https://doi.org/10.1016/j.rsma.2022.102659>
- Cullen, J. J. (2015). Subsurface chlorophyll maximum layers: enduring enigma or mystery solved? *Annual Review of Marine Science*, 7, 207-239. <https://doi.org/10.1146/annurev-marine-010213-135111>
- Defriez, E. J., Sheppard, L. W., Reid, P. C., & Reuman, D. C. (2016). Climate change related regime shifts have altered spatial synchrony of plankton dynamics in the North Sea. *Global Change Biology*, 22(6), 2069-2080. <https://doi.org/10.1111/gcb.13229>
- Fennel K, Boss E. (2003). Subsurface maxima of phytoplankton and chlorophyll: steady-state solutions from a simple model. *Limnol. Oceanogr.* 48:1521 <https://doi.org/10.4319/lo.2003.48.4.1521>
- Franks, P. J. (2002). NPZ models of plankton dynamics: their construction, coupling to physics, and application. *Journal of Oceanography*, 58(2), 379-387. <https://doi.org/10.1023/A:1015874028196>
- Gittings, J.A., Raitsos, D.E., Krokos, G. et al. (2018). Impacts of warming on phytoplankton abundance and phenology in a typical tropical marine ecosystem. *Sci Rep* 8, 2240

<https://doi.org/10.1038/s41598-018-20560-5>

https://elischolar.library.yale.edu/journal_of_marine_research/419

- Global Modeling and Assimilation Office (GMAO) (2015). MERRA-2 instM_2d_lfo_Nx: 2d,Monthly mean,Instantaneous,Single-Level,Assimilation,Land Surface Forcings V5.12.4, Greenbelt, MD, USA, Goddard Earth Sciences Data and Information Services Center (GES DISC), Accessed: [Accessed: August 20, 2021], 10.5067/11F99Y6TXN99
- Gregg, W. and Rousseaux, C. (2017). NASA Ocean Biogeochemical Model assimilating satellite chlorophyll data global monthly VR2017, Edited by Watson Gregg and Cecile Rousseaux, Greenbelt, MD, USA, Goddard Earth Sciences Data and Information Services Center (GES DISC), Accessed: [Accessed: August 20, 2021], 10.5067/BHCFDIICIU5
- Hinsley, W., Field, T., Woods, J. (2007). Creating Individual Based Models of the Plankton Ecosystem. In: Shi, Y., van Albada, G.D., Dongarra, J., Sloot, P.M.A. (eds) Computational Science – ICCS 2007. ICCS 2007. Lecture Notes in Computer Science, vol 4487. Springer, Berlin, Heidelberg. https://doi.org/10.1007/978-3-540-72584-8_15
- Huisman, J., Pham Thi, N., Karl, D. et al. (2006). Reduced mixing generates oscillations and chaos in the oceanic deep chlorophyll maximum. *Nature*, 439, 322–325 <https://doi.org/10.1038/nature04245>
- Intergovernmental Panel on Climate Change (2014). Climate Change 2014: Synthesis Report. Contribution of Working Groups I, II and III to the Fifth Assessment Report of the Intergovernmental Panel on Climate Change [Core Writing Team, R.K. Pachauri and L.A. Meyer (eds.)]. IPCC, Geneva, Switzerland, 151 pp.
- Jagadeesan, L., Jyothibabu, R., Arunpandi, N. et al. (2017). Copepod grazing and their impact on phytoplankton standing stock and production in a tropical coastal water during the different seasons. *Environ Monit Assess*, 189, 105 <https://doi.org/10.1007/s10661-017-5804-y>
- Lewandowska, A. M., Hillebrand, H., Lengfellner, K., & Sommer, U. (2014). Temperature effects on phytoplankton diversity—The zooplankton link. *Journal of Sea Research*, 85, 359–364. <https://doi.org/10.1016/j.seares.2013.07.003>
- Li, G., Lin, Q., Ni, G., Shen, P., Fan, Y., Huang, L., & Tan, Y. (2012). Vertical patterns of early summer chlorophyll a concentration in the Indian Ocean with special reference to the variation of deep chlorophyll maximum. *Journal of Marine Biology*. <https://doi.org/10.1155/2012/801248>
- Li, Q. P., & Hansell, D. A. (2016). Mechanisms controlling vertical variability of subsurface chlorophyll maxima in a mode-water eddy. *Journal of Marine Research*, 74(3), 175–199.
- Lien, R.-C., Ma, B., Lee, C. M., Sanford, T. B., Mensah, V., Centurioni, L. R., Cornuelle, B. D., Gopalakrishnan, G., Gordon, A. L., Chang, M.-H., Jayne, S. R., & Yang, Y. J. (2015). The Kuroshio and Luzon Undercurrent East of Luzon Island. *Oceanography*, 28(4), 54–63. <http://www.jstor.org/stable/24861928>
- Liu, C. C., & Woods, J. D. (2004). Prediction of ocean colour: Monte Carlo simulation applied to a virtual ecosystem based on the Lagrangian Ensemble method. *International Journal of Remote Sensing*, 25(5), 921–936. <https://doi.org/10.1080/0143116031000139809>
- Lopez-Urrutia, A. and Moran, X.A. (2015) . Temperature affects the size-structure of phytoplankton communities in the ocean *Limnol. Oceanogr.* 60, 2015, 733–738 <https://doi.org/10.1002/lno.10049>
- Maranón, E., Cermeno, P., Latasa, M., & Tadonlélé, R. D. (2012). Temperature, resources, and phytoplankton size structure in the ocean. *Limnology and Oceanography*, 57(5), 1266–1278. <https://doi.org/10.4319/lo.2012.57.5.1266>
- Marinov, I., Doney, S. C., & Lima, I. D. (2010). Response of ocean phytoplankton community structure to climate change over the 21st century: partitioning the effects of nutrients, temperature and light. *Biogeosciences*, 7(12), 3941–3959. <https://doi.org/10.5194/bg-7-3941-2010>
- McQuatters-Gollop, A., Reid, P., Edwards, M., Burkill, P., Castellani, C., Batten, S., Gieskes, W., Beare, D., Bidigare, D., Head, E., Johnson, R., Kahru, M. Koslow, K., Pena, A. (2011) . Is there a decline in marine phytoplankton?. *Nature* 472, E6–E7 <https://doi.org/10.1038/nature09950>
- Mesquita, M. C., Prestes, A. C. C., Gomes, A. M., & Marinho, M. M. (2020). Direct effects of temperature on growth of different tropical phytoplankton species. *Microbial ecology*, 79(1), 1–11.
- Miller, C., Lynch, D. R., Carlotti, F., Gentleman, W., & Lewis, C. V. W. (1998). Coupling of an individual-based population dynamic model of *Calanus finmarchicus* to a circulation model for the Georges Bank region. *Fisheries Oceanography*, 7, 219–234. <https://doi.org/10.1046/j.1365-2419.1998.00072.x>
- Morán, X. A. G., A. López-Urrutia, A. Calvo-Díaz, and W. K. W. Li. (2010) . Increasing importance of small phytoplankton in a warmer ocean. *Glob. Chang. Biol.* 16: 1137–1144. <https://doi.org/10.1111/j.1365-2486.2009.01960.x>
- Nogueira, E., Woods, J. D., Harris, C., Field, A. J., & Talbot, S. (2006).

- Phytoplankton co-existence: Results from an individual-based simulation model. *Ecological Modelling*, 198(1), 1-22. <https://doi.org/10.1016/j.ecolmodel.2006.04.013>
- O'Connor, M.I., Piehler, M.F., Leech, D.M., Anton, A., Bruno, J.F., (2009). Warming and resource availability shift food web structure and metabolism. *PLoS Biology* 7 (8). <https://doi.org/10.1371/journal.pbio.1000178>
- Pannard, A., Planas, D., & Beisner, B. E. (2015). Macrozooplankton and the persistence of the deep chlorophyll maximum in a stratified lake. *Freshwater Biology*, 60(8), 1717-1733. <https://doi.org/10.1111/fwb.12604>
- Peter KH, Sommer U (2012). Phytoplankton Cell Size: Intra- and Interspecific Effects of Warming and Grazing. *PLoS ONE* 7(11): e49632. <https://doi.org/10.1371/journal.pone.0049632>
- Probyn, T. A., B. A. Mitchell-Innes, and S. Searson. (1995). Primary productivity and nitrogen uptake in the subsurface chlorophyll maximum on the eastern Agulhas Bank. *Cont. Shelf Res.*, 15(15), 1903–1920. [https://doi.org/10.1016/0278-4343\(94\)00099-9](https://doi.org/10.1016/0278-4343(94)00099-9)
- Qiu, B., Rudnick, D. L., Ceroveck, I., Cornuelle, B. D., Chen, S., Schönau, M. C., McClean, J. L., & Gopalakrishnan, G. (2015). The Pacific North Equatorial Current: New Insights from the Origins of the Kuroshio and Mindanao Currents (OKMC) Project. *Oceanography*, 28(4), 24–33. <http://www.jstor.org/stable/24861925>
- Rasconi, S., Winter, K., & Kainz, M. J. (2017). Temperature increase and fluctuation induce phytoplankton biodiversity loss—Evidence from a multi-seasonal mesocosm experiment. *Ecology and Evolution*, 7(9), 2936-2946. <https://doi.org/10.1002/ece3.2889>
- Richardson TL, Jackson GA. (2007). Small phytoplankton and carbon export from the surface ocean. *Science*. 315(5813):838-40. <https://doi.org/10.1126/science.1133471>
- Righetti, D., Vogt, M., Gruber, N., Psomas, A., & Zimmermann, N. E. (2019). Global pattern of phytoplankton diversity driven by temperature and environmental variability. *Science advances*, 5(5). <https://doi.org/10.1126/sciadv.aau6253>
- Riley, G. A., Stommel, H. & Bumpus, D. F. (1949). Quantitative ecology of the plankton of the western North Atlantic. *Bull. Bingham Oceanogr. Coll.*, Vol. 12, No. 3, pp. 1-169
- Sinerchia, M., Field, A. J., Woods, J. D., Vallergera, S., & Hinsley, W. R. (2012). Using an individual-based model with four trophic levels to model the effect of predation and competition on squid recruitment. *ICES Journal of Marine Science: Journal du Conseil*, 69(3), 439-447. <https://doi.org/10.1093/icesjms/fsr190>
- Sommer, U., and Lewandowska, A. (2011). Climate change and the phytoplankton spring bloom: warming and overwintering zooplankton have similar effects on phytoplankton. *Glob. Change Biol.* 17, 154–162. <https://doi.org/10.1111/j.1365-2486.2010.02182.x>
- Takahashi, M., & Hori, T. (1984). Abundance of picophytoplankton in the subsurface chlorophyll maximum layer in subtropical and tropical waters. *Marine Biology*, 79(2), 177–186. <https://doi.org/10.1007/bf00951826>
- Talley, L. D. (2007), Hydrographic Atlas of the World Ocean Circulation Experiment (WOCE). Volume 2: Pacific Ocean, edited by M. Sparrow, P. Chapman, and J. Gould, Int. WOCE Proj. Off., Southampton, U. K
- Taucher, J., & Oschlies, A. (2011). Can we predict the direction of marine primary production change under global warming?. *Geophysical Research Letters*, 38(2). <https://doi.org/10.1029/2010GL045934>
- Thomas, M. K., Kremer, C. T., Klausmeier, C. A., & Litchman, E. (2012). A global pattern of thermal adaptation in marine phytoplankton. *Science*, 338(6110), 1085-1088. <https://doi.org/10.1126/science.1224836>
- Thomas, M. K., Aranguren-Gassis, M., Kremer, C. T., Gould, M. R., Anderson, K., Klausmeier, C. A., & Litchman, E. (2017). Temperature-nutrient interactions exacerbate sensitivity to warming in phytoplankton. *Global Change Biology*, 23(8), 3269–3280. <https://doi.org/10.1111/gcb.13641>
- Uitz, J., H. Claustre, A. Morel, and S. B. Hooker (2006). Vertical distribution of phytoplankton communities in open ocean: An assessment based on surface chlorophyll, *J. Geophysical Research.*, 111, C08005, <https://doi.org/10.1029/2005JC003207>
- Weston, K., Fernand, L., Mills, D.K., Delahunty, R. and Brown, J. (2005). Primary production in the deep chlorophyll maximum of the central North Sea. *Journal of Plankton Research*, 27(9), pp.909-922. <https://doi.org/10.1093/plankt/fbi064>
- Wolf, K. U., & Woods, J. D. (1988). Lagrangian simulation of primary production in the physical environment—the deep chlorophyll maximum and nutricline. In *Toward a theory on biological-physical interactions in the World ocean*. Springer, Dordrecht.
- Woods, J. D. (2005). The Lagrangian Ensemble metamodel for simulating plankton ecosystems. *Progress in Oceanography*, 67(1), 84-159. <https://doi.org/10.1016/j.pocean.2005.04.003>

- Woods, J. D., & Barkmann, W. (1995). Modelling oligotrophic zooplankton production: Seasonal oligotrophy off the Azores. *ICES Journal of Marine Science*, 52, 723–734. [https://doi.org/10.1016/1054-3139\(95\)80085-9](https://doi.org/10.1016/1054-3139(95)80085-9)
- Woods, J. D., & Onken, R. (1982). Diurnal variation and primary production in the ocean preliminary results of a Lagrangian ensemble model. *Journal of Plankton Research*, 4(3), 735-756. <https://doi.org/10.1093/plankt/4.3.735>
- Woods, J. D., Perilli, A., & Barkmann, W. (2005). Stability and predictability of a Virtual Plankton Ecosystem created by an individual-based model. *Progress in Oceanography*, 67, 1-2:43-83. <https://doi.org/10.1016/j.pocean.2005.04.004>
- Xiu, P., Chai, F., Curchitser, E.N. (2018). Future changes in coastal upwelling ecosystems with global warming: The case of the California Current System. *Science Reports* 8, 2866 <https://doi.org/10.1038/s41598-018-21247-7>